

# FIBRE REINFORCED ALKALI- ACTIVATED ROCK WOOL

MAJDA PAVLIN, BARBARA HORVAT, VILMA DUCMAN

Slovenian National Building and Civil Engineering Institute, Ljubljana, Slovenia  
majda.pavlin@zag.si, barbara.horvat@zag.si, vilma.ducman@zag.si

**Abstract** Mineral wool, i.e. rock and glass wool, represents considerable challenge after its functional-time runs out due to its small density leading to large volume consumption during transport and in landfills where it usually ends. Because rock wool is mineralogically and chemically a promising precursor material for alkali-activation, it was milled from few centimetres-decimeters long fibres to micron-sized fibres. Since fibres in alkali-activated materials generally show an increase in mechanical strength, especially the bending strength, 1 m% of additional fibres (basalt, cellulose (2 types), glass, polypropylene, polyvinyl alcohol and steel fibres) was used in the alkali mixture, that was cured at 40 °C for 3 days. Time dependence of the mechanical strengths of alkali-activated materials with and without additional fibres was followed. Maximal increase of compressive and bending strength after 28 days was reached with polypropylene fibres, i.e. it was 20% and 30% higher than compressive and bending strength of alkali-activated material without additional fibres respectively.

**Keywords:**

waste mineral  
wool,  
fibre,  
alkali-activated  
material,  
mechanical  
strength,  
upcycling

## 1 Introduction

Mineral wool (rock/stone, glass and slag wool) is a material consisting of fibres and shots, where shots did not fiberize before solidification. The less the shots mineral wool contains, the better it's quality (Brane Sirok et al., 2008). Newer production technologies add on fibres' surface different organic resins as the binder to modify mineral wool's compressive, bending and tensile strengths (Kowatsch, 2010). Yearly global production of the mineral wool is increasing with the average annual rate of 1.8% since 2013 and has reached 19M tonnes in 2019 ("The Global Mineral Wool Market Started to Slow Down - Global Trade Magazine," n.d.), while the yearly amount of mineral wool's waste in Austria is 20-30K tonnes (Sattler et al., 2020). When predicted that mineral wool waste is approximately linked to the number of inhabitants, mineral wool waste in all EU countries together is then 1M-1.5M tonnes yearly. Therefore it is crucial to solve the problem of waste mineral wool disposal due to its large volume consumption during transport and in landfills.

One way for use of the waste mineral wool is using it as a precursor in alkali activation, where milled mineral wool reacts with alkali and forms aluminosilicate matrix, in which not-reacted fibres get completely immobilized (Horvat et al., 2018). Alkali activation idea was 1<sup>st</sup> reported in a patent in 1895, whereas the precursor was proposed blast-furnace slag and as activator the caustic soda with slaked lime (Whiting, 1895). But only in last decade researchers started to test also some other precursors than metakaolin, slag and fly-ash, i.e. refractory materials, foundry sand and other foundry wastes (Horvat et al., 2019), waste green ceramics (Horvat and Ducman, 2019) and last years also waste mineral wools where glass wool had higher compressive strength than rock wool (Yliniemi et al., 2016). All these materials can be used in alkali activation because they contain big enough amount of amorphous Al and Si, which are present in the matrix in the tetrahedron formation with O-bridges. To compensate electric charge of Al in the tetrahedron, elements of the 1<sup>st</sup> and 2<sup>nd</sup> group are needed, i.e. the positive ions either come from the precursor if it contains them in the amorphous phase, or from the alkali activator (Horvat and Ducman, 2019).

In many materials, additional mechanical reinforcement is achieved with the addition of fibres made from different materials and of different sizes and shapes, i.e. in polymer composites (Navin Chand, 2008), metal and ceramic matrix composites (Eckold, 1994), civil engineering composites (Harris, 2005), syntactic foams (Sydney H. Goodman and Hanna Dodiuk-Kenig, 2014) etc.

The purpose of presented work is to evaluate the effect of several different fibres (basalt, cellulose, glass, polypropylene, polyvinyl alcohol and steel fibres) on mechanical strengths in alkali activated pulverized waste rock wool.

## **2 Materials and Methods**

### **2.1 Analysis of precursor, additives and alkali-activated materials**

Rock wool waste (RW) (Horvat et al., 2018), labelled 17 09 041, was collected from Termit. RW was 1<sup>st</sup> manually cleaned of all large impurities, cut into smaller pieces, and milled in a concrete mixer by using steel balls (27 pieces, 47.5 mm in diameter), every kilogram of RW for 2.5 hours (coarse RW). The milled sample was dried at 105 °C for 24 hours and sieved below 63 µm. The residue was ground in the homogenizer (powder mixer shaker, Turbola T2F) in 2 l plastic container with steel balls (50 pieces of diameter 9.8 mm) and sieved below 63 µm (fine RW).

The particle size of coarse and fine RW was measured by particle size and shape analyzer (Microtrac MRB, SYNC).

Fibres were used from previous projects: basalt (B), cellulose (fibres (CF) and fibres squeezed into thin cubes (CC)), glass (G), polypropylene (PP), polyvinyl alcohol (PVA) and steel fibres (S).

Chemical analysis of RW was performed using X-ray fluorescence (XRF; Thermo Scientific ARL Perform'X Sequential XRF) on melted discs of the mixture of ignited RW powder (sieved below 63 µm) and Fluxana<sub>(s)</sub> (FX-X50-2, lithium tetraborate 50% / lithium metaborate 50% is used to lower melting point) with the addition of a few drops of LiBr<sub>(l)</sub> (prepared from 50 ml H<sub>2</sub>O and 7.5 g of LiBr<sub>(s)</sub> from Acros Organics, which is used to avoid sticking of the melt to the platinum vessel). Obtained data were characterized by software UniQuant 5.

Mineralogical characterization of RW powder (sieved below 63  $\mu\text{m}$ ) was performed with X-ray powder diffraction (XRD; Empyrean PANalytical X-ray Diffractometer, Cu X-ray source) and software X'Pert Highscore plus 4.1. Rietveld refinement with an external standard (a pure  $\text{Al}_2\text{O}_3$  crystal) was used to estimate the amount of amorphous phase and minerals.

Scanning electron microscope (SEM; Jeol JSM-IT500) under low vacuum conditions was used to investigate surface, shape, size and microstructure of non-sputtered RW, fibres and/or alkali-activated materials.

Bending and compressive strength of alkali-activated fibreless and fibre reinforced samples were measured with compression and bending strength testing machine (ToniTechnik ToniNORM) at age 3 and 28 days.

Alkali-activated samples' geometric density was determined by weighting the sample and dividing its mass by its volume.

## 2.2 Preparation of alkali-activated samples

RW as precursor and fibres used as additional reinforcement in alkali-activated synthesis are shown in Fig. 1. RW that was used in alkali-activation was prepared in the same manner as for XRF and XRD analysis, i.e. milled and sieved below 63  $\mu\text{m}$ , while dry fibres were used as received.



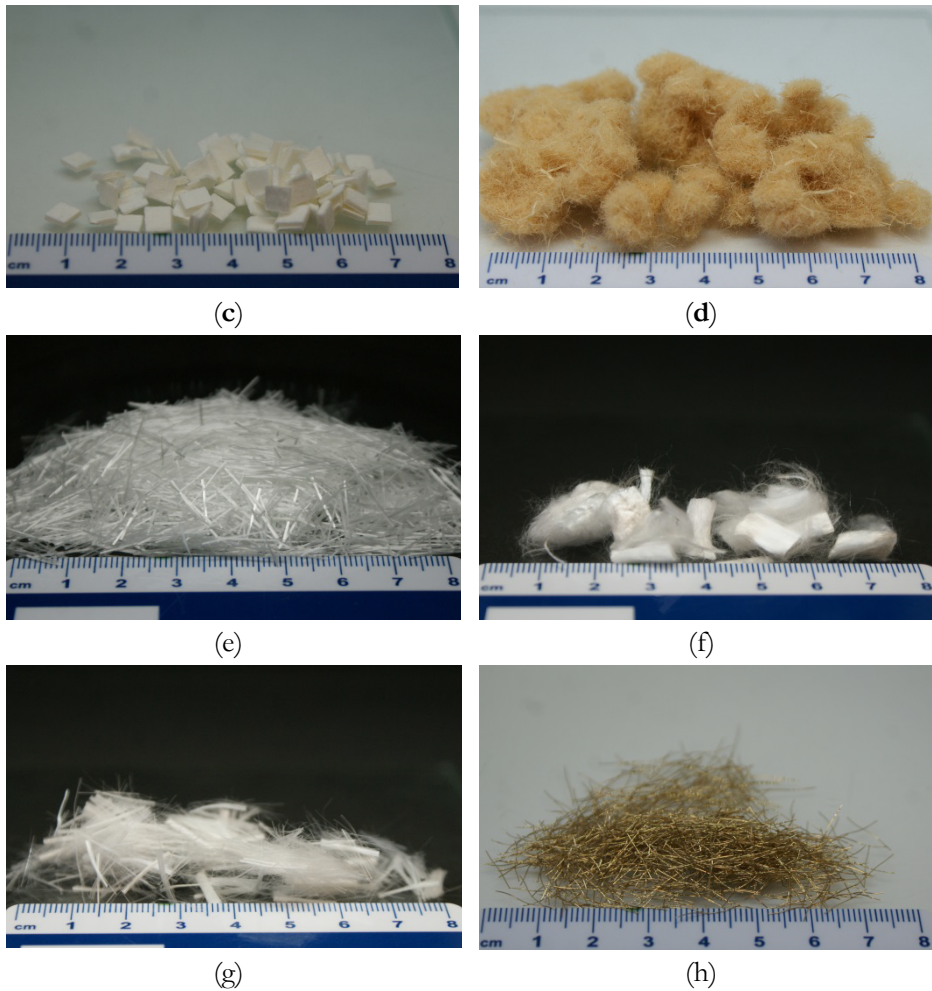


**Figure 1: Photograph of (a) milled and sieved RW (on the inset is original RW), and fibres: (b) basalt, (c) cellulose fibres, (d) cellulose cubes, (e) glass fibres, (f) polypropylene fibres, (g) polyvinyl alcohol fibres, and (h) steel fibres.**

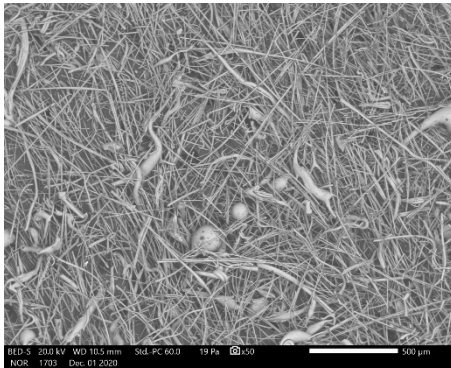
Source: own.

As alkali-activator, only Na-water glass (Silvez, mining company Termit, with the mass percentage of  $\text{Na}_2\text{O}$  12.8%, and mass percentage of  $\text{SiO}_2$  29.2%) was used. Alkali slurry was prepared in mass ratio RW : Na-water glass : fibre = 100 : 95 : 0/1, moulded into rubber-silicon moulds measuring (80x20x20) mm<sup>3</sup> and cured in drying chamber (WTB Binder) at 40 °C for 3 days.

### 3 Results and discussion

#### 3.1 Analysis of precursor

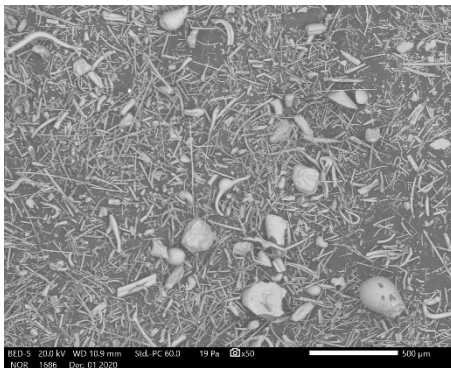
SEM micrographs of RW that was not milled (original RW), that was milled (coarse RW), and that was milled for so long that it could be sieved below  $63\ \mu\text{m}$  (fine RW) are presented in Fig. 2 (a, b, c respectively). Particle size analysis of coarse and fine RW is presented in Fig. 3.



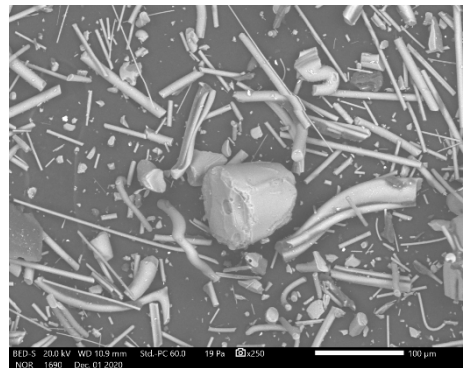
(a)



(b)



(c)



(d)

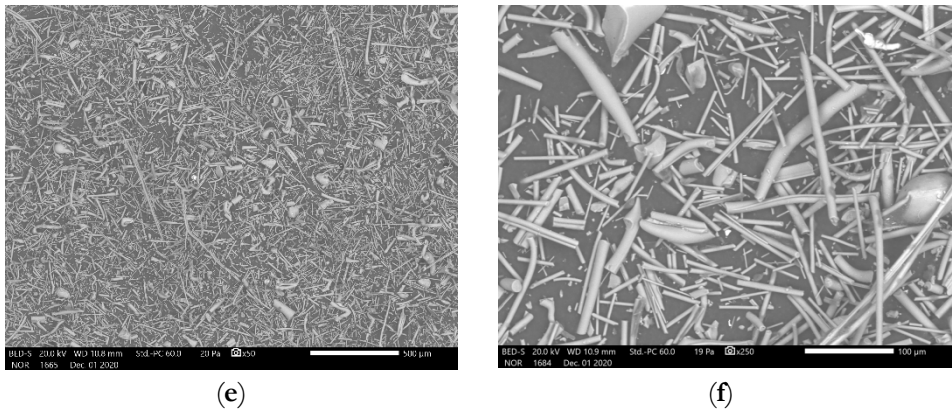


**Figure 2:** SEM micrographs of not milled RW [(a) magnification 50x, (b) magnification 250x], milled RW [(c) magnification 50x, (d) magnification 250x], milled and sieved below 63  $\mu\text{m}$  RW [(e) magnification 50x, (f) magnification 250x].

Source: own.

RW, even if milled and sieved below 63  $\mu\text{m}$ , keeps an elongated cylindrical shape (Fig. 2). With 1<sup>st</sup> step milling long thin fibres are broken into smaller pieces (Fig. 2 (a) to (c)), while “stones” stay intact until the sample is milled so long that it can be fully sieved below 63  $\mu\text{m}$  (Fig. 2 (c) to (e)). The milling effect can be seen also in Fig. 3, where red line represents material after 1<sup>st</sup> step milling and the blue line represents material that was milled and sieved under 63  $\mu\text{m}$ . Both prepared samples are fine-grained, i.e. more than 50% of all material is smaller from 75  $\mu\text{m}$ : 50% of coarse RW grains are below or equal to 52  $\mu\text{m}$ , while 50% of fine RW grains are smaller or equal to 31  $\mu\text{m}$ . Coefficient of uniformity for coarse RW is 6.7, while for fine RW is 4.8. Coefficient of curvature on the other hand is for coarse RW 0.8, while for fine RW is a bit higher than 1.0. For the well-graded material coefficient of uniformity should be bigger from 1, and the coefficient of curvature between 1 and 3, meaning that only fine RW is well graded. Therefore in alkali-activation, only RW that was milled and sieved below 63  $\mu\text{m}$  was used as a precursor.

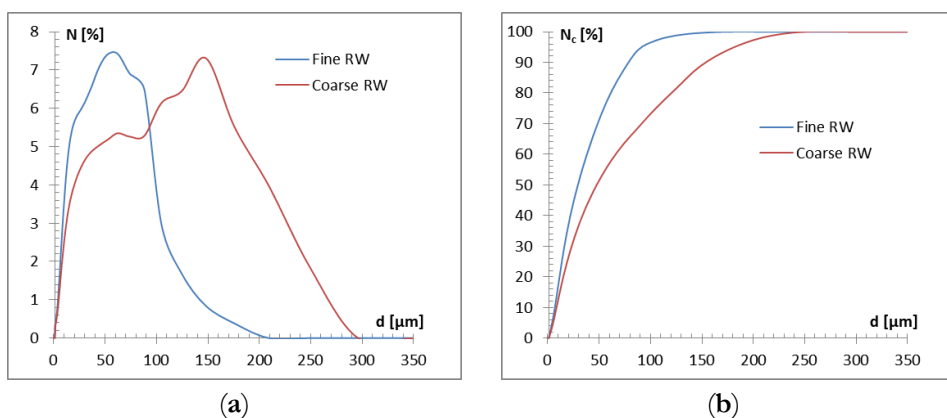
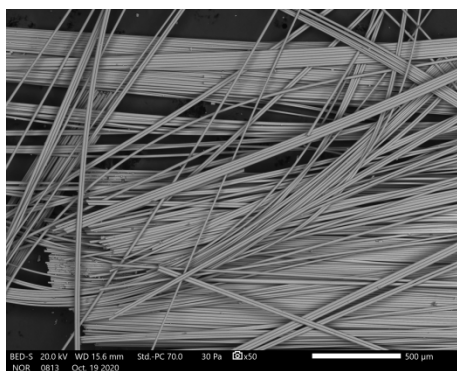


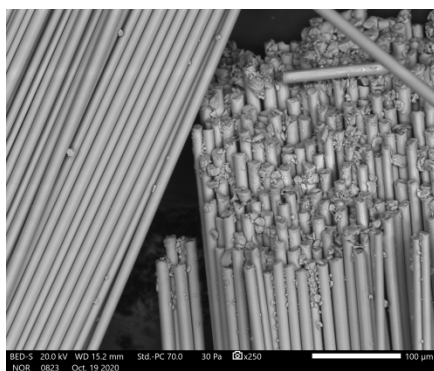
**Figure 3: (a) Particle size distribution, (b) cumulative particle size distribution of coarse RW (red line), and fine RW (blue line).**

Source: own.

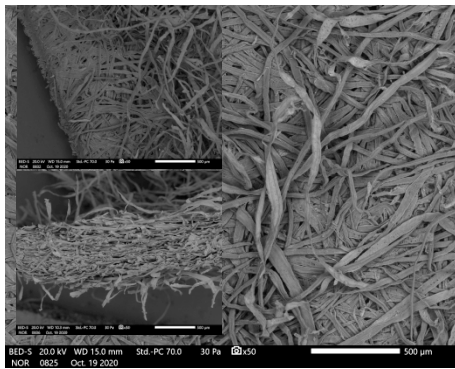
All fibres used in alkali-activation to gain higher bending and compressive strength are presented in Fig. 4. Natural fibres are from cellulose (Fig. 4 (c) to (f), CC and CF), while all the rest are completely artificial (B, G, PP, PVA and S). Several of them are found ordered in larger groups: B, G and PVA; without any specific order is CF, PP, and also S (which is present in alkali-activated synthesis just as few fibres due to its higher density); while CC is squeezed into thin cubes with random orientation of cellulose fibres.



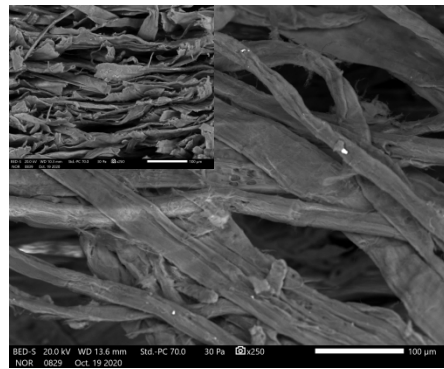
(a)



(b)



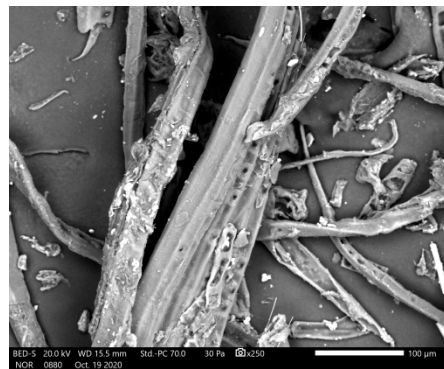
(c)



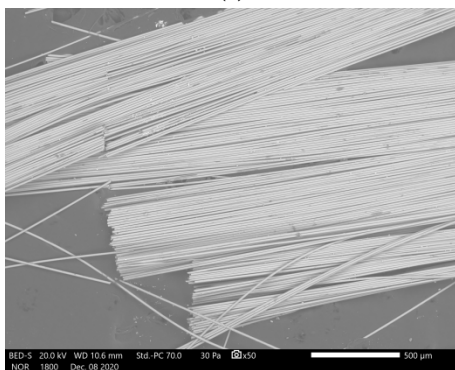
(d)



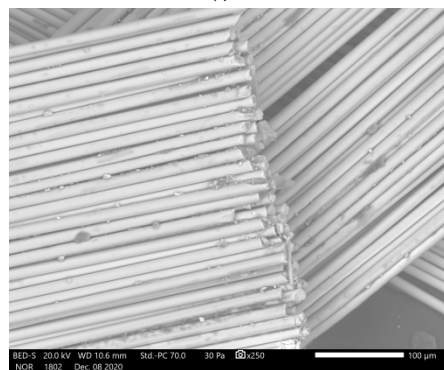
(e)



(f)



(g)



(h)

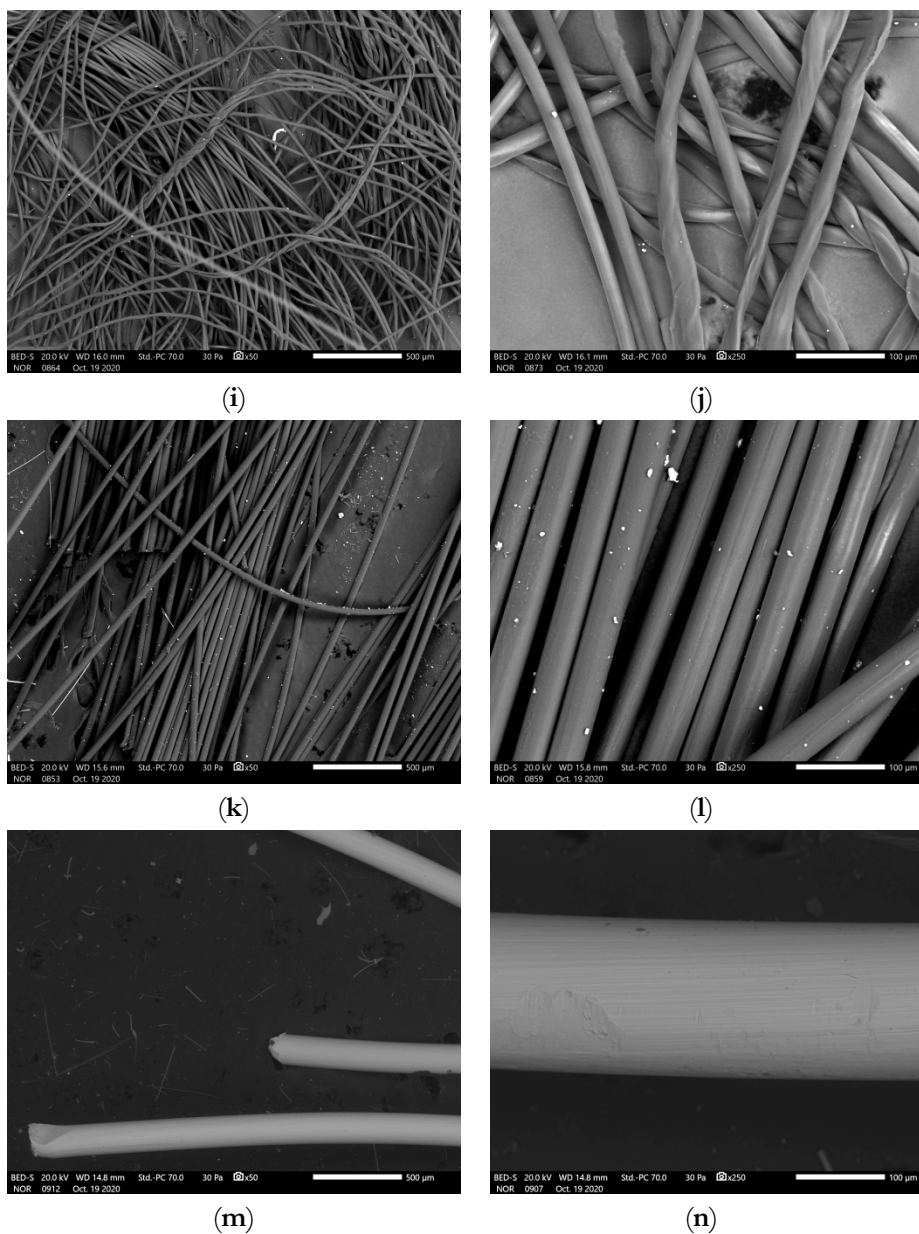


Figure 4: SEM micrographs of fibers at 50x (left) and 250x (right) magnification: B [(a), (b)], CC [(c), (d)], CF [(e), (f)], G [(g), (h)], PP [(i), (j)], PVA [(k), (l)], and S [(m), (n)].

Source: own.

XRF chemical analysis of RW is presented in 1<sup>st</sup> row in Table 1, XRD mineralogical analysis is in its 2<sup>nd</sup> row of Table 1, wherein crystalline phase only small amount of quartz was present (determined by Rietveld refinement), and in the 3<sup>rd</sup> line of Table 1 elements' mass percentages in the amorphous phase are calculated as the difference between the XRF and XRD results.

**Table 1: Chemical (XRF) and mineralogical (XRD) analysis of RW.**

Precursor	Elements/m%	Na	K	Cs	Mg	Ca	Sr	Ba	Al	Si
RW	XRF	1.5	0.2	0	6.3	11.6	0	0	8.6	18.9
	XRD	0	0	0	0	0	0	0	0	0.1
	XRF-XRD	1.5	0.2	0	6.3	11.6	0	0	8.6	18.8

According to the literature (Duxson et al., 2005) for reaching the highest compressive strength most promising ratio Na, Al and Si present in AAM is 1:1:1.9. In our previous work (Horvat and Ducman, 2019) this model was tested and upgraded to be able to compare the amorphous amount of whole 1<sup>st</sup> and 2<sup>nd</sup> group to Al and Si, to predict also potential future efflorescence. For used RW ratio of the amount of substance between (1<sup>st</sup> : 2<sup>nd</sup> : Al : Si) is (0.2: 1.7 : 1 : 2.1). If no element from the 2<sup>nd</sup> group participates in the reaction, efflorescence can be avoided by the addition of elements from 1<sup>st</sup> group with NaOH without changing the amount of Si, or with Na-water glass were the amount of Si rises and could compromise the final mechanical strength as a side effect.

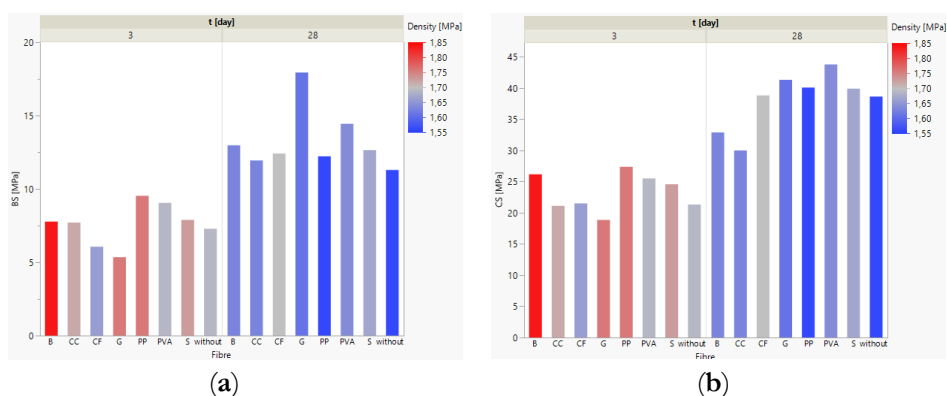
### 3.2 Analysis of alkali-activated samples

The compressive and bending strength of 3 and 28 days old alkali-activated RW with and without fibres is presented in Table 2 and Fig. 5.

Mechanical strengths of all alkali-activated samples with and without fibres increase with time while their density decreases due to the evaporation of water, i.e. shrinking has a smaller effect than the mass loss. At the same time, chemical reactions (besides physical evaporation of water) are still going on and creating strong chemical bonds in the matrix. These bonds more than just compensate the negative effects of the evaporation that result in crack formation in the matrix (which can be seen on micrographs of alkali-activated materials presented on Fig. 6).

**Table 2: Compressive and bending strengths of alkali-activated samples with their geometrical densities after 3 and 28 days (presented on one decimal).**

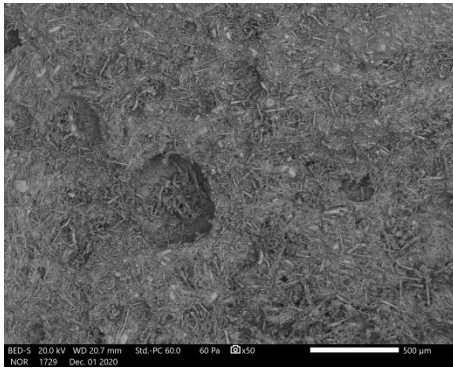
Fibre	Compressive strength/ MPa		Bending strength/ MPa		Density/ kg/l	
	3 days	28 days	3 days	28 days	3 days	28 days
/	21.3	38.6	7.3	11.3	1.7	1.6
B	26.2	32.9	7.8	13.0	1.8	1.6
CC	21.1	30.0	7.7	12.0	1.7	1.6
CF	21.5	38.8	6.1	12.4	1.7	1.7
G	18.1	41.3	5.4	17.9	1.8	1.6
PP	27.4	40.1	9.5	12.2	1.8	1.6
PVA	25.5	43.8	9.1	14.5	1.7	1.6
S	24.6	39.9	7.9	12.7	1.7	1.7

**Figure 5: (a) Bending and (b) compressive strength of alkali activated RW with and without fibres.**

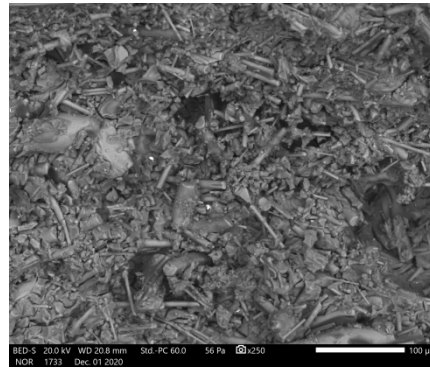
Source: own.

All fibres used in alkali-activation of RW increased the bending strengths of 28-days old material, while for compressive strengths this is true only for G, PP, PVA and S, while other fibres either decreased its value (B, CC) or had no influence (CF). Highest reached BS after 28 days had a sample with G fibres (17.9 MPa was BS, while CS reached 41.3 MPa), while highest CS after 28 days had sample with PVA fibres (43.8 MPa was CS, while BS reached 14.5 MPa), i.e. CS and BS for samples containing G fibres was 10% and 60% higher than values for reference respectively, while CS and BS for samples containing PVA fibres was 20% and 30% bigger from alkali-activated RW without additional fibres.

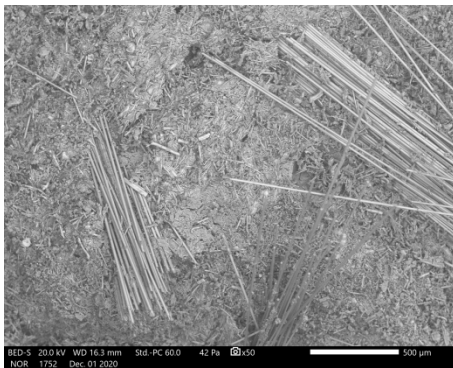
SEM micrographs of alkali-activated samples with and without fibres are presented on Fig. 6. Matrix of alkali-activated RW did not change with the addition of fibres, because none reacted with alkali and did not change the chemical reaction. All samples had spherical pores (organic resin present on RW reacts with alkali and releases gasses, which get trapped into the matrix when matrix gets too viscose for the bubble to be able to travel out from the slurry with the difference of densities; Fig. 6 (a)) and 1-dimensional cracks which are a consequence of physical evaporation of water while drying (Fig. 6 with magnification 250).



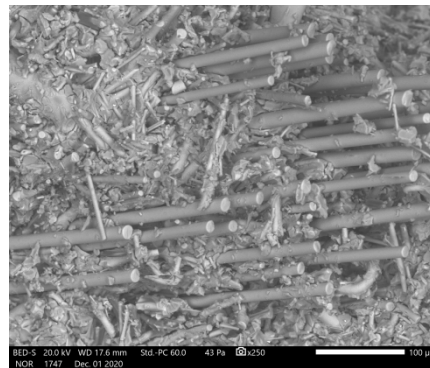
(a)



(b)



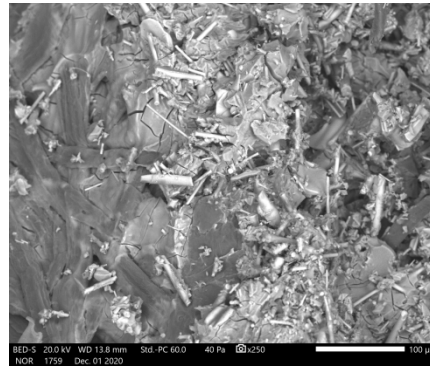
(c)



(d)



(e)



(f)



(g)



(h)



(i)



(j)

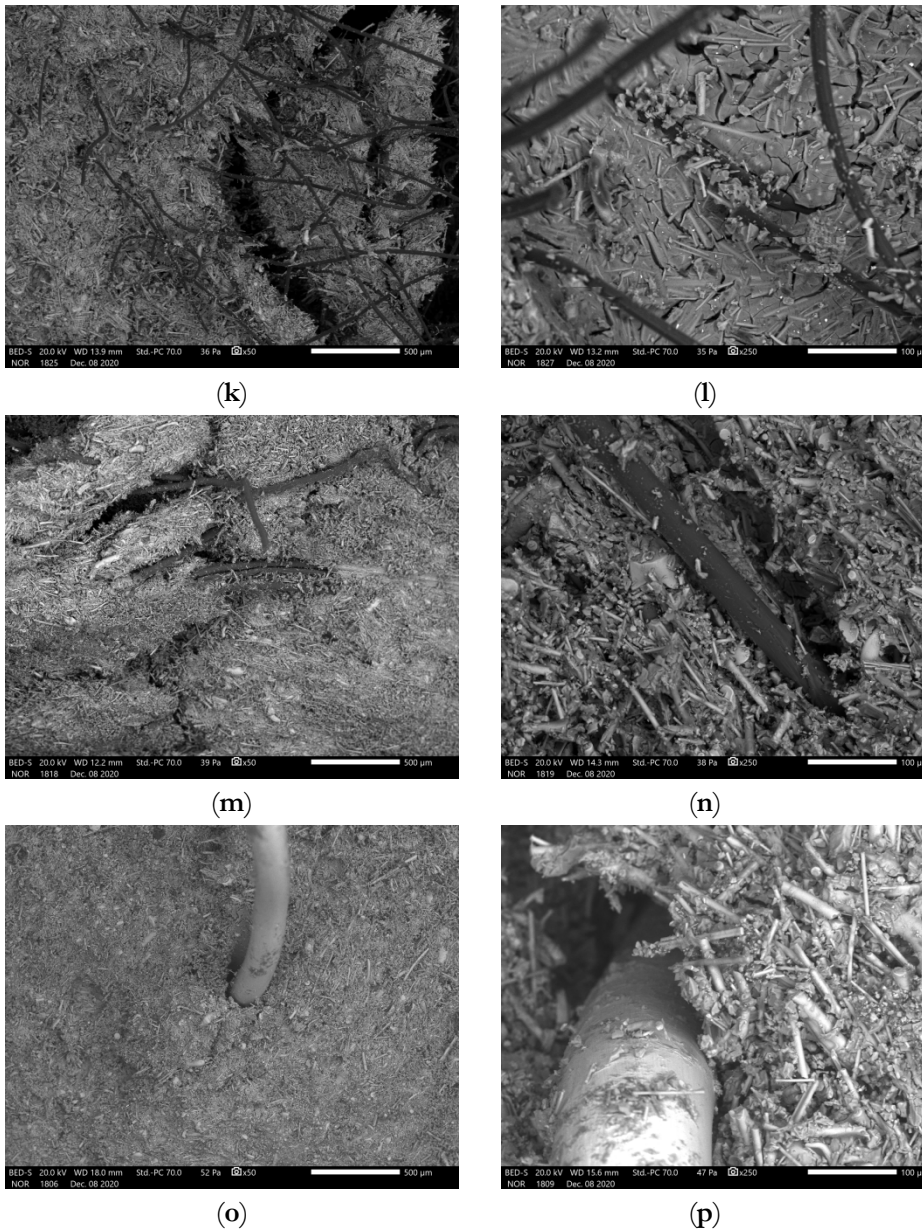


Figure 6: SEM micrographs of alkali-activated RW at 50x (left) and 250x (right) magnification without additional fibres [(a), (b)], and with additional fibres: B [(c), (d)], CC [(e), (f)], CF [(g), (h)], G [(i), (j)], PP [(k), (l)], PVA [(m), (n)], and S [(o), (p)].

Source: own.

To determine the optimal amount of added fibres further investigation is needed, where focus would be also on the number of fibres (through density and mass), their geometry (approximate diameter and length) and their whole surface area present in the alkali-activated material.

## 4 Conclusions

The results show that the addition of fibres is beneficial for bending strength, while compressive strength increased only with the addition of glass, polypropylene, polyvinyl alcohol and steel fibres, while other fibres left the compressive strength either intact, or even lowered it. Most promising among all samples, that increased both mechanical strengths, was a sample with added polyvinyl alcohol fibres (bending strength increased for 20%, while compressive strength for 30%), while addition of glass fibres resulted in overall biggest increase of bending strength (60%).

## Acknowledgements

Project No. C3330-17-529032 “Raziskovalci-2.0-ZAG-529032” was granted by Ministry of Education, Science and Sport of the Republic of Slovenia. The investment is co-financed by the Republic of Slovenia, Ministry of Education, Science and Sport and the European Regional Development Fund. WOOL2LOOP project received funding from the European Union’s Horizon 2020 research and innovation programme under grant agreement No 821000. Slovenian Research Agency supported Programme Group P2-0273.

The Metrology Institute of the Republic of Slovenia is acknowledged for the use of XRF.

Cooperation with Termit d.d. and Mrs Alenka Sešek Pavlin from Termit d.d. is highly appreciated.

## References

- Brane Sirok, Bogdan Blagojevic, Peter Bullen, 2008. Mineral Wool Production and Properties. Woodhead Publishing.
- Duxson, P., Provis, J.L., Lukey, G.C., Mallicoat, S.W., Kriven, W.M., van Deventer, J.S.J., 2005. Understanding the relationship between geopolymer composition, microstructure and mechanical properties. *Colloids and Surfaces A: Physicochemical and Engineering Aspects* 269, 47–58. <https://doi.org/10.1016/j.colsurfa.2005.06.060>
- Eckold, G., 1994. Design and manufacture of composite structures. Woodhead, Cambridge.
- Harris, B., 2005. Fatigue in Composites: Science and Technology of the Fatigue Response of Fibre-Reinforced Plastics 870.
- Horvat, B., Češnovar, M., Pavlin, A., Ducman, V., 2018. Upcycling with alkali activation technology, in: *Technologies & Business Models for Circular Economy*. Presented at the 1st International Conference on Technologies & Business Models for Circular Economy, Univerzitetna založba Univerze v Mariboru / University of Maribor Press, pp. 261–272. <https://doi.org/10.18690/978-961-286-211-4.22>

- Horvat, B., Ducman, V., 2019. Potential of Green Ceramics Waste for Alkali Activated Foams 30.
- Horvat, B., Pavlin, A.S., Ducman, V., 2019. Foundry wastes as potential precursor in alkali activation technology, in: *Technologies & Business Models for Circular Economy*. Presented at the 2nd International Conference on Technologies & Business Models for Circular Economy, Univerzitetna založba Univerze v Mariboru / University of Maribor Press.
- Kowatsch, S., 2010. Mineral Wool Insulation Binders, in: Pilato, L. (Ed.), *Phenolic Resins: A Century of Progress*. Springer Berlin Heidelberg, Berlin, Heidelberg, pp. 209–242. [https://doi.org/10.1007/978-3-642-04714-5\\_10](https://doi.org/10.1007/978-3-642-04714-5_10)
- Navin Chand, 2008. *Tribology of Natural Fiber Polymer Composites*. Woodhead Publishing.
- Sattler, T., Pomberger, R., Schimek, J., Vollprecht, D., 2020. MINERAL WOOL WASTE IN AUSTRIA, ASSOCIATED HEALTH ASPECTS AND RECYCLING OPTIONS. *Detritus* 174–180. <https://doi.org/10.31025/2611-4135/2020.13904>
- Sydney H. Goodman, Hanna Dodiuk-Kenig, 2014. *Handbook of Thermoset Plastics*, Third. ed. William Andrew.
- The Global Mineral Wool Market Started to Slow Down - Global Trade Magazine [WWW Document], n.d. URL <https://www.globaltrademag.com/the-global-mineral-wool-market-started-to-slow-down/> (accessed 12.19.20).
- Whiting, J., 1895. *Manufacture of Cement*. 544706.
- Yliniemi, J., Kinnunen, P., Karinkanta, P., Illikainen, M., 2016. Utilization of Mineral Wools as Alkali-Activated Material Precursor. *Materials* 9, 312. <https://doi.org/10.3390/ma9050312>

